Biomacromolecules

Article

pubs.acs.org/Biomac

Grafting of Bacterial Polyhydroxybutyrate (PHB) onto Cellulose via In Situ Reactive Extrusion with Dicumyl Peroxide

Liqing Wei,[†] Armando G. McDonald,*[,†] and Nicole M. Stark[‡]

[†]Renewable Materials Program, Department of Forest, Rangeland and Fire Sciences, University of Idaho, Moscow, Idaho 83844-1132, United States

[‡]U.S. Department of Agriculture, Forest Service, Forest Products Laboratory, One Gifford Pinchot Drive, Madison, Wisconsin 53726-2398, United States

Supporting Information

ABSTRACT: Polyhydroxybutyrate (PHB) was grafted onto cellulose fiber by dicumyl peroxide (DCP) radical initiation via in situ reactive extrusion. The yield of the grafted (cellulose-*g*-PHB) copolymer was recorded and grafting efficiency was found to be dependent on the reaction time and DCP concentration. The grafting mechanism was investigated by electron spin resonance (ESR) analysis and showed the presence of radicals produced by DCP radical initiation. The grafted copolymer structure was determined by nuclear magnetic resonance (NMR) spectroscopy. Scanning electronic microscopy (SEM) showed that the cellulose-*g*-PHB copolymer formed a continuous phase between the surfaces of cellulose and PHB as compared to cellulose-PHB blends. The relative crystallinity of cellulose and PHB were quantified from Fourier transform infrared (FTIR) spectra and X-ray diffraction (XRD) results, while the absolute degree of crystallinity was evaluated by differential scanning calorimetry (DSC). The reduction of crystallinity indicated the grafting reaction occurred not just in the amorphous region but also slightly in crystalline regions of both cellulose and PHB. The smaller crystal sizes suggested the brittleness of PHB was decreased. Thermogravimetric analysis (TGA) showed that the grafted copolymer was stabilized relative to PHB. By varying the reaction parameters the compositions (%PHB and %cellulose) of resultant cellulose-*g*-PHB copolymer are expected to be manipulated to obtain tunable properties.

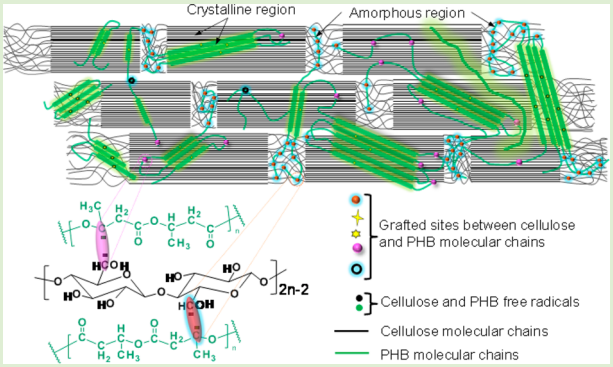

INTRODUCTION

Cellulose is the most abundant naturally occurring biopolymer and has received a great deal of attention due to its good mechanical properties, chemical reactivity, and being a renewable resource.[1,2] The physical and chemical properties of cellulose greatly depend on its specific structure. Cellulose is a homopolymer of repeating 1 → 4 glycosidic linked β-D-glucopyranose units.[3] The hydroxyl groups on cellulose contribute to the high chemical reactivity of the glucopyranosyl rings and also tend to form extensive intra- and intermolecular C−H···O hydrogen bonds.[2,4] The hydrogen bonding is responsible for the crystalline nature of cellulose fibers resulting in its high tensile strength (∼18 GPa) and modulus (∼138 GPa).[5] The properties of cellulose make it a suitable reinforcement in biocomposite materials when the density of that is not a concern and become an attractive environmentally friendly material toward a sustainable/green society.[5−7] Meantime, the lack of thermoplasticity and highly hydrophilicity make it not desirable for some applications.

Great efforts have been carried out to modify the properties of cellulose by imparting the desired and targeted properties of polymers onto cellulose (or its derivatives) through the method, namely "grafting copolymerization". The graft copolymerization approaches are summarized into two classes, "grafting-onto" and "grafting-from".[1,2] The later strategy, such as the ring-opening copolymerization of poly(lactic acid) (PLA) or poly(ε-caprolactone) (PCL) with cellulose,[8,9] radical (irradiation initiation) initiated by in situ polymerization of monomer onto cellulose,[10−12] and ion-initiated polymerization,[13,14] has been extensively studied and reported. However, the former strategy is scarcely studied due to the low reactivity of solid cellulose and relatively low grafting density, and the characterization is difficult.[1,2]

Polyhydroxybutyrate (PHB) and polyhydroxybutyrate-*co*-hydroxyvalerate (PHBV) are the two major members of the polyhydroxyalkanoate (PHA) family, known for good biodegradability, biocompatibility, and being bioderived from renewable resources by bacterial synthesis.[15,16] Therefore, PHA have been used for biomedical applications including tissue engineering and bone replacement materials and also

Received: January 13, 2015
Revised: February 6, 2015
Published: February 9, 2015

ACS Publications © 2015 American Chemical Society

DOI: 10.1021/acs.biomac.5b00049
Biomacromolecules 2015, 16, 1040−1049

Scheme 1. General Mechanism of Peroxide Radical Initiated Grafting of PHB onto Cellulose

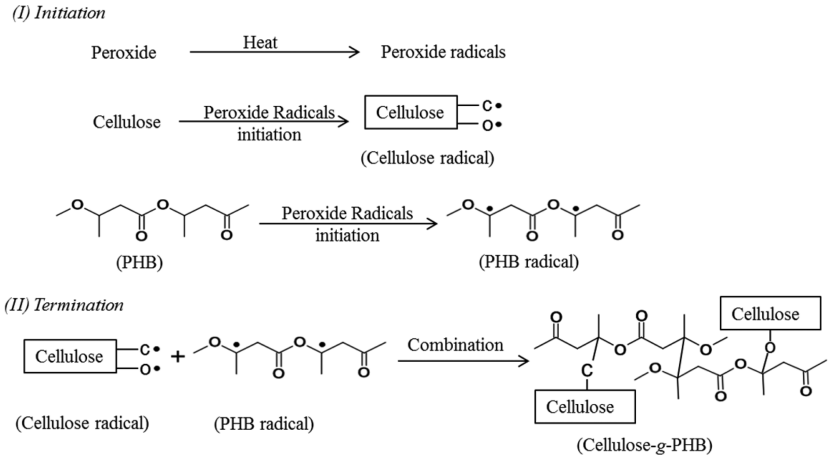

used in packaging materials and personal disposable articles.[15,17] However, PHAs have some drawbacks, such as poor melt strength, low thermal stability, and relatively high brittleness and production cost.[17] Our previous work using dicumyl peroxide to initiate the cross-linking of PHB between tertiary carbon radicals found this method is successful to improve the melting processability and thermal stability, and meantime to reduce the crystallinity of the resultant cross-linked PHB by long-chain branching.[18] The degree of crystallinity was reduced significantly via this method; whereas documentation of grafting PHAs onto cellulose via grafting copolymerization is scarce. Samain and co-workers prepared PHA grafted onto cellulose by first transforming PHA into lower molecular weight oligomers (telechelic diols) and converted them into chloride oligomers which were then grafted onto cellulose in solution.[19] Hence, developing an alternative grafting method which can easily be incorporated into an industrial process (e.g., extrusion) to retain their intrinsic properties, and enhance the compatibility between the polymer phases, triggered the research interest of this study.

In this work, low concentrations of dicumyl peroxide (DCP) radicals were generated at higher temperature and performed as initiator to graft PHB onto cellulose powder via in situ reactive extrusion. Grafting parameters were calculated to evaluate the effects of reaction time and DCP concentration on the yield of grafted products. The radicals produced and chemical structures of resultant grafted copolymer were characterized by ESR and nuclear NMR spectroscopies, respectively, to investigate the possible grafting mechanism. FT-IR spectroscopy and XRD were used to investigate the crystallinity changes due to grafting, while thermal properties were characterized by DSC and TGA. The morphology of the polymeric materials was examined by SEM.

■ EXPERIMENTAL SECTION

Materials. Commercial cellulose fiber (CF1: Ø, 15−30 μm; length, 124−400 μm, Whatman), polyhydroxybutyrate (PHB: M_w = 290000 g/mol, Tianan Biopolymer Inc., China), dicumyl peroxide (DCP) (98%, Sigma-Aldrich, U.S.A.), trifluoroacetic anhydride (TFAA, Oakwood Products, U.S.A.), acetone (99.5%, Macron Fine Chemicals, U.S.A.), $CHCl_3$ (J.T. Baker, U.S.A.), and $CDCl_3$ (D: 99.8%; Cambridge Isotope Laboratories. Inc., U.S.A.) were used as received.

Preparation of CF1-*g*-PHB and CF1-PHB Blend. Vacuum dried PHB and CF1 were separately coated with DCP in acetone (4−8 mg/mL) for 30 min. To limit the formation of PHB homopolymers (Scheme 1) a smaller portion of DCP was coated onto PHB as compared to CF1.

PHB (80%, 1.6 g) and CF1 (20%, 0.40 g) were dried and premixed in a beaker, resulting in a total DCP content between 2 and 5% (Table S1, available in the Supporting Information). The CF1-*g*-PHB copolymer was prepared in a Dynisco Lab Mixer Molder/Extruder (LMM) by the reactive extrusion process. The blended materials were placed in the LMM at 175 °C and mixed for a defined period of reaction time (t_R, 5−15 min) and then extruded into strands (1 mm Ø) or injection molded into rectangular bars (60 × 9 × 2 mm^3). Blends of CF1 and PHB (CF1-PHB, without addition of DCP) were prepared as control strand and rectangular bar samples. The reaction time was optimized. The extruded copolymerized strands were Soxhlet extracted with $CHCl_3$ for 24 h to dissolve any nonreacted PHB, and then filtered through a nylon screen to collect the crude gel products. The pore size of the screen was about 450 μm which was sufficient to allow the nonreacted CF1 to pass through, and the gel left on the screen was considered to be the true CF1-*g*-PHB copolymer. The gel was vacuum-dried and gel yield (gel%) was calculated from

$$\text{gel\%} = W_{\text{drygel}}/W_0 \times 100 \quad (1)$$

where W_{drygel} and W_0 are the dry weights of the isolated copolymer gel and the strand samples before extraction, respectively. The t_R will be optimized based on maximum gel% and that time will be called t_{max}.

Grafting Parameters. The graft percentage (%GP), weight percent of grafted polymer with respect to initial weight of cellulose; the graft efficiency (%GE), weight % of PHB grafted onto cellulose backbone; and weight conversion (%WC), weight % of cellulose grafted were calculated as follows:

$$\text{\%GP} = (W_{\text{gf}} - W_{\text{CF1}})/W_{\text{CF1}} \times 100 \quad (2)$$

$$\text{\%GE} = (W_{\text{gf}} - W_{\text{CF1}})/W_{\text{PHB}} \times 100 \quad (3)$$

$$\text{\%WC} = W_{\text{gf}}/W_{\text{PHB}} \times 100 \quad (4)$$

where W_{gf}, W_{CF1}, and W_{PHB} are the weights of the grafted copolymer recovered after Soxhlet extraction, initial CF1, and PHB weights.

ESR Spectroscopy. Radicals present in cellulose and PHB were studied by ESR spectroscopy (Bruker EMX Plus Spectrometer (X-band)). Extruded strands were immediately placed in liquid nitrogen and ground in a mortar and particles transferred into an ESR tube standing in liquid nitrogen. ESR spectra were recorded at room temperature after thawing the samples. The instrumental parameters were as follows: microwave power, 2 mW; microwave frequency, 9.87 GHz; modulation frequency, 100 kHz; time constant, 5 ms. Data were acquired and processed using WinEPR software.

Acetylation of CF1 and CF1-*g*-PHB. CF1 (1 g) and CF1-*g*-PHB (1 g) were acetylated with acetic acid (1 mL) and TFAA (2 mL) at 50 °C for overnight. The acetylated CF1 and CF1-*g*-PHB products were

DOI: 10.1021/acs.biomac.5b00049
Biomacromolecules 2015, 16, 1040−1049

precipitated out with cold ethanol, filtered, and dried under vacuum until constant weight.

NMR Spectroscopy. Acetylated CF1 and CF1-*g*-PHB samples were dissolved in $CDCl_3$, and ^1H, ^{13}C NMR, DEPT-135, and $^1H-^{13}C$ HSQC spectra were recorded on an Advance Bruker 500 MHz spectrometer at 27 °C. TMS was used as the internal reference for chemical shift. Spectra were analyzed using SpinWorks v3.1.7 software.

Scanning Electron Microscopy. The copolymerized CF1-*g*-PHB and CF1-PHB blend bar samples were microtomed into 100 μm thick specimens and lightly coated with carbon (bottom layer) and gold (surface layer) and analyzed at 3−4.5 kV at 500× on a LEO Gemini field emission SEM.

X-ray Diffraction. CF1, PHB and ground CF1-*g*-PHB samples were characterized by XRD (Siemens D5000 diffractometer). The system was set up with a rotating Cu Kα2 X-ray tubes operating at 40 kV with a current density of 30 mA at room temperature. Scanning was performed over the 2θ ranging from 5 to 50° with steps of 0.2°. The diffractograms were analyzed using IGOR Pro v6 software. The crystallinity index of cellulose CF1 (CrI_{CF1}) was determined from the ratio of the integral intensities of crystalline portions to the total intensity of sample according to the method of Segal et al.:[20]

$$CrI_{CF1} = (1 - (I_{am}/I_{002})) \times 100 \quad (5)$$

where I_{am} is the intensity of the peak at 2θ = 18° and I_{002} is the maximum intensity of the (002) plane diffraction.

The PHB crystallinity index was calculated according to

$$CrI_{PHB} = I_{17}/I_{total} \times 100 \quad (6)$$

where I_{17} is the intensity of the peak close to 2θ = 17° and I_{total} is the total intensity of all crystalline peaks of PHB.

The crystal size dimension D_{hkl} was evaluated by Scherrer's formula:[21]

$$D_{hkl} = K \times \lambda/(\beta_{1/2} \times \cos\ \theta) \quad (7)$$

where K is the crystal shape constant, λ is the X-ray wavelength (λ = 0.1542 nm), $\beta_{1/2}$ is the peak full width at half of maxima intensity (fwhm = 2 deg.) obtained by IGOR Pro, when peak fitting was conducted with Gaussian function, and θ is the diffraction angle.

FTIR Spectroscopy. CF1, PHB, and CF1-*g*-PHB were characterized by FTIR spectroscopy using a Thermo Nicolet iS5 FTIR spectrometer (ZnSe attenuated total reflection (ATR) probe (iD5)). Samples (in triplicate) were analyzed after vacuum drying. The absorbance spectra were averaged and baseline corrected using Omnic v9.0 software (Thermo Scientific).

Total crystallinity index (TCI) of CF1, the PHB carbonyl index ($I_{PHB/C=O}$) and PHB crystallinity index ($I_{PHB/C-O}$) of PHB before and after grafting were calculated as follows:

$$TCI = A_{1370}/A_{2900} \quad (8)$$

$$I_{PHB/C=O} = A_{1720}/A_{1740} \quad (9)$$

$$I_{PHB/C-O} = A_{1230}/A_{1453} \quad (10)$$

where A_{1370} and A_{2900} are the areas of cellulose CF1 peaks at 1370 and 2900 cm^{-1}, respectively, and A_{1230}, A_{1453}, A_{1720}, and A_{1740} are the areas of the peaks at 1230, 1453, 1720, and 1740 cm^{-1} from PHB molecular chains, respectively. All band areas were determined by peak fitting processing using IGOR Pro software.[22] Gaussian functionality was employed for peak fitting using a peak width at half height value of 19 cm^{-1}.

Thermal Analysis. DSC was performed using a TA Instruments model Q200 DSC with refrigerated cooling. The samples were (i) equilibrated at 40 °C (3 min) then ramped to 180 °C at 10 °C/min, held isothermally for 5 min to remove any thermal history, (ii) cooled to −50 °C at the rate of −10 °C/min and held isothermally for 3 min, and (iii) reheated to 180 °C at 10 °C/min to record the heating scan. Data were analyzed using TA Universal Analysis v4.4A software.

TGA was conducted using a PerkinElmer TGA-7 instrument at a heating rate of 10 °C/min under nitrogen atmosphere (30 mL/min). The energy of activation for the decomposition of samples will be calculated with fraction (α) decomposed at different temperatures from the differential TGA (DTG) results based on the equation:[14]

$$\ln(1 - \alpha)^{-1} = 100E_a/(RT_s^2)/(T_f - T_i)(\theta) + C \quad (11)$$

where T_i and T_f are the initial and final decomposition temperatures and have been taken as points of deviation from baseline in the DTG curve above the dehydration temperature. The θ is the difference of decomposition temperature (T) and temperature of reference (T_s). The plot between the reciprocal of the double logarithmic ($1 - \alpha$) versus temperature deference ($T - T_s$) enabled calculation of the value of activation energy of the sample.

RESULTS AND DISCUSSION

Reaction Time Optimization and Grafting Efficiency. The CF1-*g*-PHB sample formulations are given in Table S1. The influence of two factors (DCP concentration and t_R) was investigated to allow us to tailor the grafting efficiency between PHB and CF1 through controlling the initiator (free peroxide radicals) density on the surface (Table S2, available in the Supporting Information). The copolymer was extracted with $CHCl_3$ to remove any nonreacted PHB or smaller homopolymers and then filtered to remove nongrafted CF1. The dry weight of the gels was recorded and the gel% calculated and used to optimize the reaction parameters (t_R and DCP concentration). The 3D plot of gel% (Figure 1), t_R, and DCP

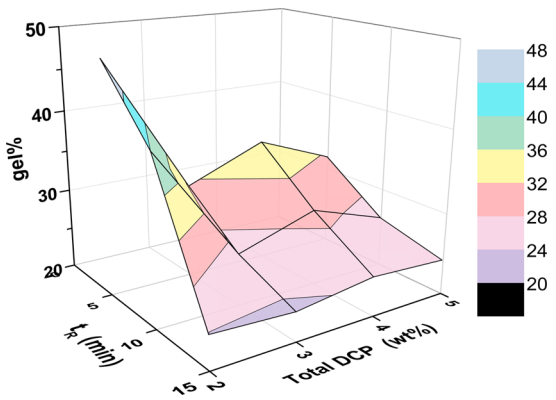

Figure 1. Effect of t_R (min) and total DCP concentration on the graft yield (gel%) of CF1 and PHB (CF1, 0.5 g; PHB, 2 g; temperature = 175 °C).

concentration showed the gel% was decreased dramatically with time (from 5 to 15 min) because the peroxide radical's half-life is short (<3 min at 175 °C).[23] The grafted sample 2CGP5 gave the highest gel content of 48% followed by 2CGP10 (gel% = 40.0), 4CGP5 (gel% = 35.3), and 5CGP5 (gel% = 31.6). Similar trends have been seen for %GP, %GE, and %WC are summarized in Table S2. The grafting efficiencies through this method were comparable to the grafting of low molecular weight PHBV onto chitosan via a condensation reaction in solvent.[24] The values of %GP, %GE, and %WC were shown to decrease with DCP concentration (>2%), indicating that the grafting takes place just majorly at the surface of cellulose and PHB. At 2% DCP sufficient quantities of radicals were available to graft PHB and CF1. Another possible explanation for this decrease in gel content with DCP concentration is that a higher level of cross-linking may occur between PHB chains than grafting between cellulose and PHB, contributing to DCP's higher mobility with PHB when melting.

DOI: 10.1021/acs.biomac.5b00049
Biomacromolecules 2015, 16, 1040−1049

Reaction Mechanism, Structure, and Morphology Characterization. From Figure 1 and Table S2 the grafting reaction primarily occurred in the first 5 min (t_{max} = 5 min), due to the short life of DCP radicals and the grafting efficiency was dependent on DCP content. Hence, a moderate peroxide content (5% DCP) was used and the grafted sample was collected at time t = 4 min ($<t_{max}$). It is worth noting that the samples collected in this way were expected to contain sufficient amounts of both cellulose and PHB radicals to be readily detected by ESR. For comparison purposes PHB + DCP (2%) and CF1 + DCP (2%) were each heated to 175 °C (4 min), then quenched in liquid nitrogen, and analyzed by ESR. Figure 2 shows the ESR spectra of radical species in PHB, CF1, and CF1-*g*-PHB (5CGP4:5% DCP and reaction for 4 min). The observation of signals confirms the free radicals were formed. The major signals of the CF1-*g*-PHB sample (Figure 2c, pointed ●) were similar to that of PHB + DCP (Figure 2a), but were of higher relative intensity (by 20%). This increase was most likely from the addition of cellulose radicals in the sample. The proposed free radical sites on PHB and CF1 based on ESR spectral analysis are shown in Figure 2d–f. For PHB, the peroxide radicals preferentially attack the tertiary protons,[25,26] which will show hyperfine splitting from 2 H_{β}s and 3 $H_{\beta'}$s; however, weak splitting (mixture of triplet + quartet, highlighted in Figure 2a,c as ○, Δ, and ⧫) were seen. As for the cellulose radical sites (Figure 2e), they are classified in two major groups: (i) carbon radicals formed on the glucopyranose ring (C_1 to C_6 positions) and (ii) alkoxy groups formed when the protons of −OH groups were abstracted.[27] Hence, the cellulose ESR spectrum showed a more complicated pattern. Whereas the weak splitting pattern of the signal centered at g = 2.003 looks like a triplet; it was therefore speculated that the C_6 radical was the dominant species (Figure 2f). Although the ESR simulations are typically used to confirm and determine the radicals environments, in this study the hyperfine coupling constant (Hfcc) could not be obtained precisely due to the weak minor signals. Furthermore, it should also point out that the radical concentration decays more rapidly at room temperature, and thus simulation was not performed. Further efforts are required to monitor the grafting reaction by ESR at high temperature (e.g., 175 °C). Therefore, ESR results confirmed the mechanism postulated in Scheme 1 that DCP radicals formed at high temperature was capable to initiate the cellulose and PHB radical formation in the solid state.

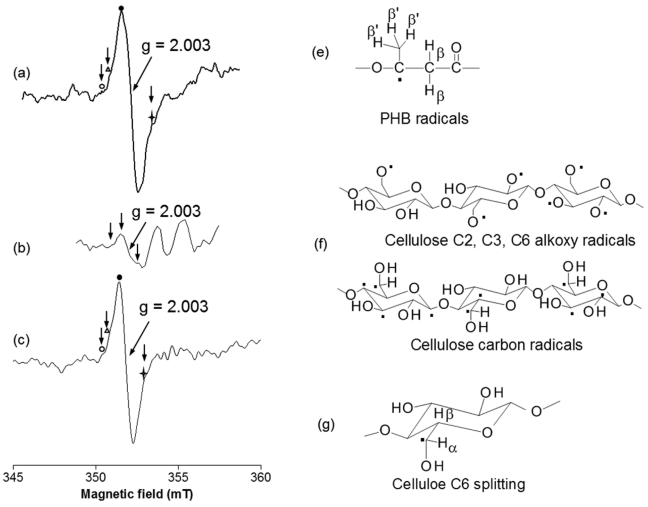

Figure 2. ESR spectra of (a) PHB + DCP (2%), (b) CF1 + DCP (2%), and (c) PHB + CF1 + DCP (5%). The peak positions are marked (major peak: ●; minor peaks: Δ, ○, and ⧫).

The chemical structures of CF1 and CF1-*g*-PHB, after acetylation, were also characterized by NMR spectroscopy. The ^{13}C NMR spectrum of acetylated CF1 (Figure 3a) showed the characteristic peaks of cellulose triacetate.[28] The signals at δ = 100.70, 72.11, 72.75, 76.30, 73.09, and 62.27 ppm were assigned to the carbons on the glucopyranosyl ring at position C_1, C_2, C_3, C_4, C_5, and C_6, respectively. The CF1-*g*-PHB sample 2CGP10 was selected for structural analysis (Figure 3b). The spectrum of acetylated 2CGP10 showed all signals of acetylated CF backbone (C_1–C_6) and C's of PHB chains at δ = 169.35, 67.84, 41.03, and 19.97 ppm corresponding to C_A, C_B, C_C, and C_D, respectively, were observed. The strong DCP radicals generated at higher temperature have strong hydrogen abstraction ability, and then could attack the cellulose at different positions, for example, to assume that OH groups attached to C_2, C_3 and C_6 are attacked alkoxy radicals ($C_2O^{\bullet}$, $C_3O^{\bullet}$, and $C_6O^{\bullet}$) will be produced, while scission of the cellulose 1,4-glycosidic bond will form alkoxy and carbon radicals ($C_4O^{\bullet}$ + $C_1^{\bullet}$), and if dehydrogenation occurred at C_1, C_5, and C_6 positions then $C_1^{\bullet}$, $C_5^{\bullet}$, and $^{\bullet}C_{6'}H$–OH radicals will be produced. Tertiary carbons (−CH) on PHB will be attacked to form $C_B^{\bullet}$ radicals. The free radicals formed on PHB and cellulose readily undergo secondary/binary terminations that new C_B–OC bonds (e.g., C_B–OC_2, C_B–OC_3, C_B–OC_4, and C_B–OC_6) and C_B–C bonds (e.g., C_B–$C_1^{\bullet}$, C_B–C_5, and C_B–$C_{6'}$HOH) will be formed. However, the −OH groups at position C_3 on cellulose are involved in intramolecular H bonding (−C_3–OH) with the pyranose ring oxygen, O_5, of the neighboring glucose ring, and similarly between −C_6–OH and O_2 of the neighboring ring. The intermolecular H bonding is formed between the hydroxyl groups on C_6 (−C_6–OH) and C_3 (−C_3–OH) of cellulose molecules that are located adjacently on the same plane.[2] These −OH groups in the crystalline regions are less likely to be accessed by radicals; in other words, only hydroxyl groups and carbons in the amorphous regions or surfaces from the crystalline region will be initiated. ^{13}C NMR spectroscopic analysis of the acetylated CF1-*g*-PHB material will help establish possible sites of grafting. Figure 3b shows the ^{13}C spectrum of acetylated CF1-*g*-PHB containing the characteristic signals for cellulose triacetate (C_1–C_6) plus signals for PHB. A new signal was observed at δ = 50.99 ppm possibly assigned to a carbon signal attached to alkoxy groups of CF1, giving a new carbon environment C–O. This newly produced carbon signal could be derived from two possible groups: (i) associated with the C_B signal of PHB position of C_B–OC_2, C_B–OC_3, C_B–OC_4, or C_B–OC_6, and therefore signal shift for grafted PHB would be observed; otherwise, (ii) contributed by $C_{6'}$ of C_B–$C_{6'}$H–OH.

To confirm the structure 2D HSQC (^1H–^{13}C) and DEPT-135 experiments were performed on acetylated 2CPG10 (Figure 4). The spectra indicated the new carbon signal (δ = 50.99 ppm) was directly attached to the strong proton signal at δ = 3.44 ppm. Furthermore, the DEPT-135 showed this carbon could be a tertiary carbon (−CH); meanwhile, only when −CH is attached to a −OH group can give the proton signal showing at such high field (δ = 3.44 ppm). To summarize these pieces of information together the chemical structure of this new carbon should be contributed by $C_{6'}$ of partial structure C_B–$C_{6'}$H–OH

DOI: 10.1021/acs.biomac.5b00049
Biomacromolecules 2015, 16, 1040–1049

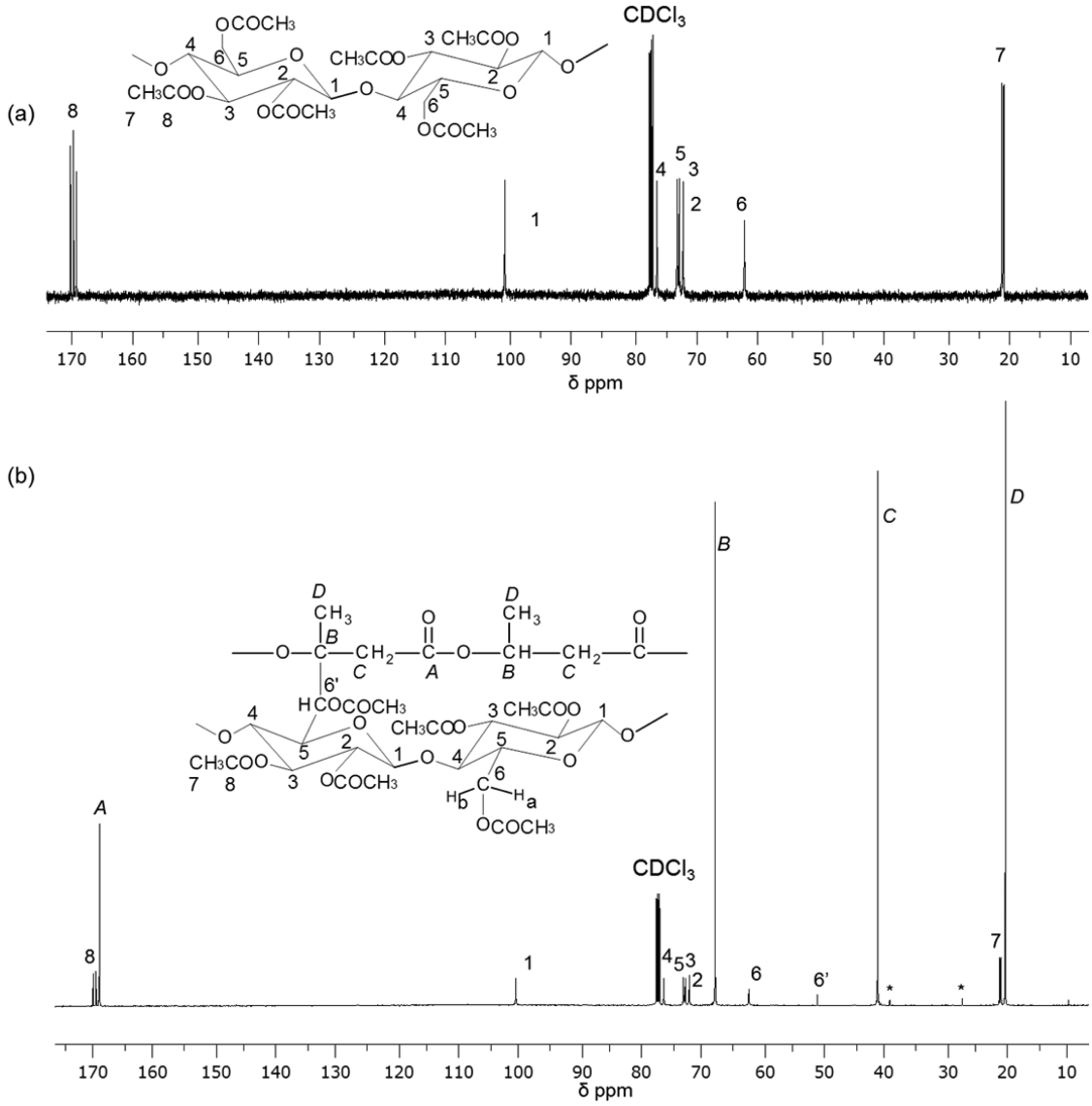

Figure 3. ^{13}C NMR spectra of (a) acetylated CF1 and (b) acetylated CF1-*g*-PHB (2CGP10). Note: the signals shown at δ = 38.9 and 27.1 ppm are from impurities of commercial PHB used (see Figure S1 in Support Information).

of the acetylated CF1-*g*-PHB (Figure 3b). This further provides evidence that one of the H's attached to C_6 of CF1 was attacked by peroxide radical that was postulated by ESR spectra (Figure 2) and then to combine with $C_B^{\bullet}$ of PHB to give the general copolymer structure (Figure 3b). This was reasonable because the atoms of $-C_6H_2-OH$ has higher flexibility/movability in comparison to C_1-C_5 of the glucopyranose ring.[29] From these results it was concluded that the in situ peroxide radicals initiated copolymerization of PHB chains onto the cellulose backbone was successful.

The SEM micrographs of the CF1 fiber showed a smooth surface (Figure 5a). After DCP treatment for 10 min (Figure 5b), the CF1 surface became slightly rougher, which may provide access for PHB to attach onto during reactive extrusion. The reactive extruded CF1-*g*-PHB (2CGP10) showed CF1 fibers encapsulated with a smooth layer of PHB suggesting that the PHB had grafted onto the cellulose surface (Figure 5c). In contrast, blends of CF1-PHB, as a nongrafted control, showed discrete zones of PHB and CF1, which was evidence of poor interfacial compatibility (Figure 5d). The literature indicated peroxide treated sisal cellulose fibers had better compatibility with a polyethylene matrix.[30]

Thermal Properties Changes Due to Grafting. The thermal stability of CF1-*g*-PHB was found to be higher than PHB and CF1-PHB blend as shown in TG and DTG curves (Figure 6). The onset temperature (T_{onset}) of degradation for the CF1-*g*-PHB (2CGP10) sample was 22° higher than that of PHB (275 °C). The T_{onset} for the CF1-PHB blend was close to PHB, and 80% of the sample degraded in the first stage contributed to the degradation of PHB, which agrees to the formulation (CF1/PHB = 1:4). This indicated the simple blending of these two materials did not improve the thermal stability of PHB. The temperature of maximum decomposition rate (T_{max}) in sample 2CGP10 was 20 °C higher than T_{max} of PHB (300 °C). During this degradation stage, PHB was completely decomposed at T = 313 °C, while about 70% of the 2CGP10 sample was degraded at $T \leq 349$ °C followed by the second stage (349−380 °C) due to the degradation of cellulose CF1 side (Figure 6: TG curves). The final decomposition temperature (T_f) of the CF1-*g*-PHB was also increased to 478 °C due to grafting. However, the 2CGP10 copolymer was less

DOI: 10.1021/acs.biomac.5b00049
Biomacromolecules 2015, 16, 1040−1049

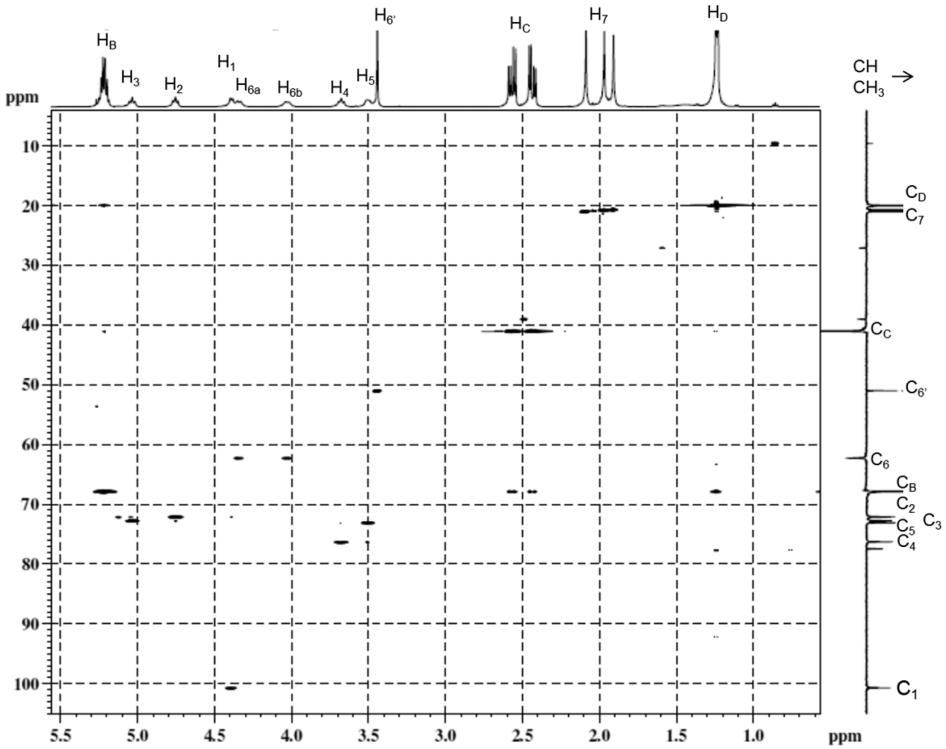

Figure 4. HSQC (^{1}H−^{13}C (DEPT-135)) spectra of acetylated CF1-*g*-PHB (2CGP10).

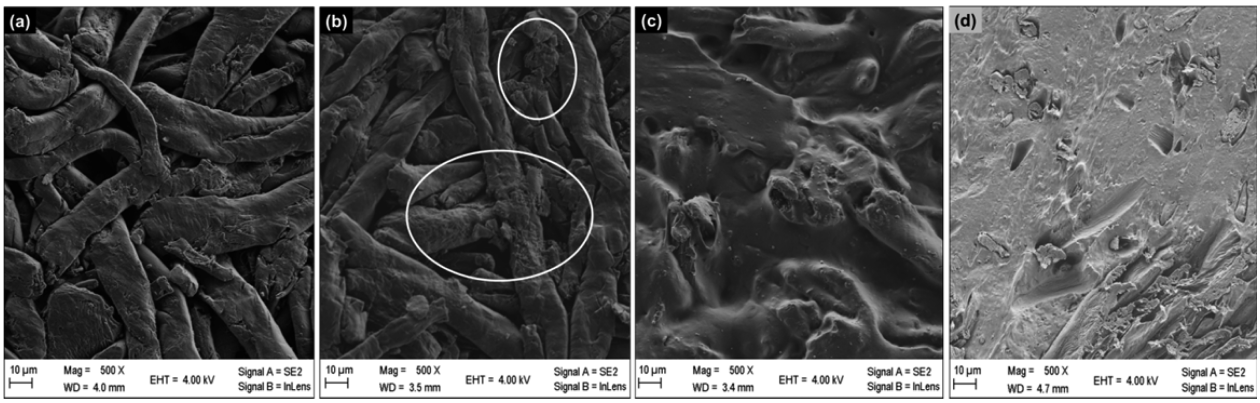

Figure 5. SEM micrographs (500×) of (a) CF1, (b) DCP treated CF1, (c) CF1-*g*-PHB (2CGP10), and (d) melt blended CF1-PHB control biocomposite.

stable than CF1, which may be attributable to having low cellulose content and some degradation or modification to the cellulose structure during grafting. As discussed above, the sample 2CGP10 only has 8% cellulose content, but showed a significantly improved thermal stability as compared to PHB, and it could be postulated that the thermal stability of the grafted copolymer was increased with the increasing of cellulose content. This was further confirmed from the activation energy of decomposition of CF1, PHB, and CF1-*g*-PHB copolymer calculated from eq 11 with decomposed fraction was obtained from DTG curves (Figure 6). The plot of $\ln[\ln(1-\alpha)^{-1}]$ versus $(T - T_s)$ is shown in Figure 7. The activation energy (E_a) of CF1-*g*-PHB was 174 kJ/mol and was higher than PHB (108 kJ/mol) and CF1-PHB blend (135 kJ/mol), but lower than cellulose (202 kJ/mol). This provided more evidence that the grafted copolymer increased the thermal stability of PHB. Through grafting more C−C bonds formed required higher energy input to activate the decomposition mechanism of the resultant copolymer.

PHB showed a glass transition (T_g) at about 4.5 °C, while the T_gs of all the CF1-*g*-PHB copolymers shifted to between 7 and 11 °C and varied slightly among samples initiated at different DCP contents. This increase in T_g was contributed to the restriction of PHB chains by the CF1 fiber surfaces and newly formed C−C bonds between amorphous PHB side chains and cellulose as well. Meantime, the ΔC_p was determined from DSC endothermic curves for each glass transition; using ΔC_p of pure PHB as a reference, the percentage of PHB (%PHB) present in the grafted copolymer was estimated by ΔC_p values (Table S3). The trend was similar to the grafting parameters results (Table S2) that 2CGP5 showed highest %PHB (88%) followed by 2CGP10 (87%), 4CGP5 (73%), 5CGP5 (69%), and 3CGP5 (60%). For the CF1-PHB blend the ΔC_p was 0.40 J g^{-1} °C^{-1}, close to 75% of the ΔC_p value of bulk PHB, which is consistent to the

DOI: 10.1021/acs.biomac.5b00049
Biomacromolecules 2015, 16, 1040−1049

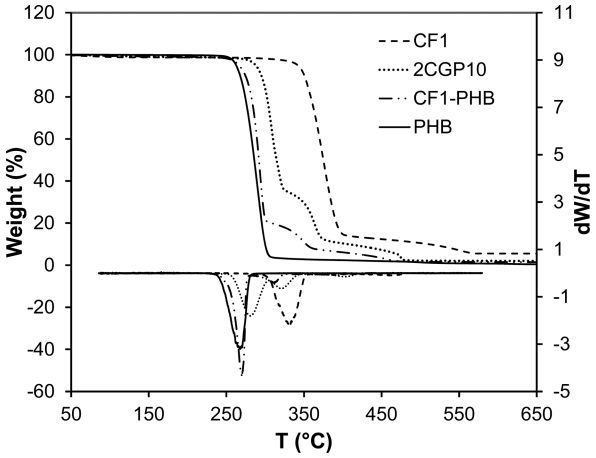

Figure 6. TGA and DTG curves of cellulose CF1, PHB, CF1-PHB blend, and CF1-*g*-PHB (2CGP10).

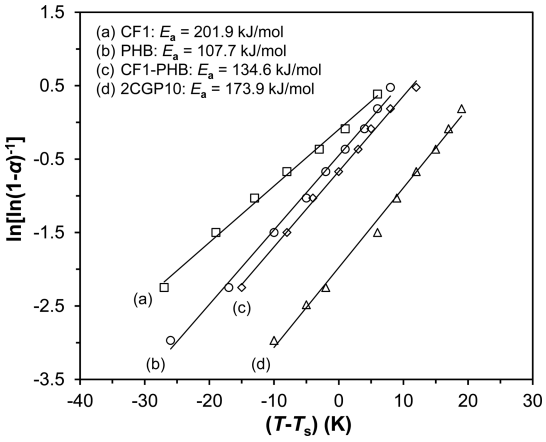

Figure 7. Plots of $\ln[\ln(1-\alpha)^{-1}]$ vs $(T - T_s)$ of CF1, PHB, CF1-PHB blend, and CF1-*g*-PHB (2CGP10) to determine their E_a from DTG data.

formulation (CF1/PHB = 1:4). This method was previously used to estimate the poly(*N*-isopropylacrylamide) content in its grafted copolymer with cellulose nanocrystals.[10] This indicated the composition of the grafted copolymer can be controlled by varying the reaction time and DCP concentration, and therefore, the thermal stability, crystallinity, and other properties are expected to be tunable.

Melting enthalpy, ΔH_m, was contributed to PHB fragment in the copolymer; hence, the melt enthalpy used for the calculation of the degree of crystallinity was normalized, and then the absolute degree of crystallinity (X_c%) was calculated (see Table S3 in the Supporting Information) according to Wei et al.[31] X_c% was lowered by grafting, indicating the PHB molecular chains aligned to form crystal structures, which were hindered either by cellulose or by the slightly long chain branching of PHB homopolymer.[18] This agrees with an increased cold crystallization temperatures (T_c) of all grafted copolymers as compared to bulk PHB. A lower X_c%, requires less energy to move the polymer chains in the amorphous phase;[32] hence, the crystallization of grafted copolymers from melts were initiated at higher temperature. However, for CF1-PHB blends a slight decrease in X_c% was observed, which would contribute to an increase of molecular motions of the amorphous phase of PHB and thus lead to a decrease in T_g. CF1-PHB blends showed double melting peaks as bulk PHB, and both of them shifted to higher temperatures, which could be attributed to the physical interaction between CF1 and PHB polymer matrix.[33] Unlike the bulk PHB and the CF1-PHB blend, only a single melting peak was observed at the lower endothermic position for all CF1-*g*-PHB copolymers. The double melting behavior was attributed to the lower stability of crystals showing at lower endothermic would recrystallize and remelt at higher temperature.[34] Therefore, the grafting of PHB onto cellulose backbone reduced the recrystallization of original crystals with lower stability or defects. These thermal properties of the resulting grafted copolymer were tunable by varying the DCP content and reaction time.

Crystallinity Changes Due to Grafting. The degree of crystallinity of polymers and composite materials significantly affect their mechanical properties and processability as well, hence, the crystalline nature of materials is important and can be obtained by a combination of FTIR and XRD techniques. Figure 8a showed the FTIR spectrum of the grafted copolymer (2CGP10) sample with characteristic absorbance peaks arising from either CF1 or PHB. The absorbance bands at 980, 1230, and 1720 cm^{-1} were assigned to crystalline PHB,[35] and intensities were reduced due to grafting. Whereas the shoulder showing at 1740 cm^{-1} of the band at 1720 cm^{-1} assigned to the carbonyl (C═O stretching) from amorphous region became more intense of grafted copolymer as compared to PHB (see Figure 8b). This observation further indicated the grafting of PHB onto cellulose hindered the crystallization of PHB from melts, resulting in more amorphous PHB. In addition, the band at 1429 cm^{-1} (symmetric $-CH_2$ bending) was characteristic of amorphous cellulose CF1, which appeared in the grafted copolymer, again supporting that grafting had occurred. The quantitative analyses of the FTIR spectra for PHB and cellulose were performed to further confirm that their crystallinity was reduced due to the grafting reaction. The spectral ratio of 1370/2900 cm^{-1} bands (total crystallinity index, TCI) was shown to be proportional to the crystallinity degree of cellulose,[36] while the band ratios 1720/1740 cm^{-1} (carbonyl index, $I_{PHB/C=O}$)[37] and 1230/1450 cm^{-1} (C−O index, $I_{PHB/C-O}$) reflect the crystallinity of PHB.[35] Quantitative analysis of the infrared crystallinity ratios calculated from the peak fitted spectra of the carbonyl region (1800−1680 cm^{-1}) for PHB and the −C−H bending (centered at 1370 cm^{-1} from crystalline region, Figure 8c) for CF1. The analyzed data for PHB, CF1, CF1-PHB blend, and CF1-*g*-PHB copolymers (2CGP5 and 2CGP10) are given in Table S4 (see Supporting Information). The incorporation of CF1 caused a reduction in PHB crystallinity of the CF1-PHB blend slightly, while grafting reduced all the three crystallinity indices significantly and these values are correlated to the graft efficiency. Grafting between cellulose and PHB acts as a coupling agent in these CF1-*g*-PHB materials, which would improve the stress transfer between the two phases.

The effect of the grafting on the crystalline structures of PHB and cellulose segments was further investigated. Vacuum dried samples were subjected to XRD analysis. The XRD diffractograms are shown in Figure 9. CF1 showed typical patterns of cellulose I; peaks showing at 2θ scale at 14.6°, 16.8°, and 22.8° were assigned to the planes of (101), (10−1), and (002), respectively. PHB had crystalline peaks at 13.7°, 16.5°, 20.2°, 21.4°, 22.4°, 25.8°, and 27.2°, respectively, corresponding to planes of (020), (110), (021), (101), (121), (040), and (200).[38] All of these peaks appeared in the CF1-PHB blends

DOI: 10.1021/acs.biomac.5b00049
Biomacromolecules 2015, 16, 1040−1049

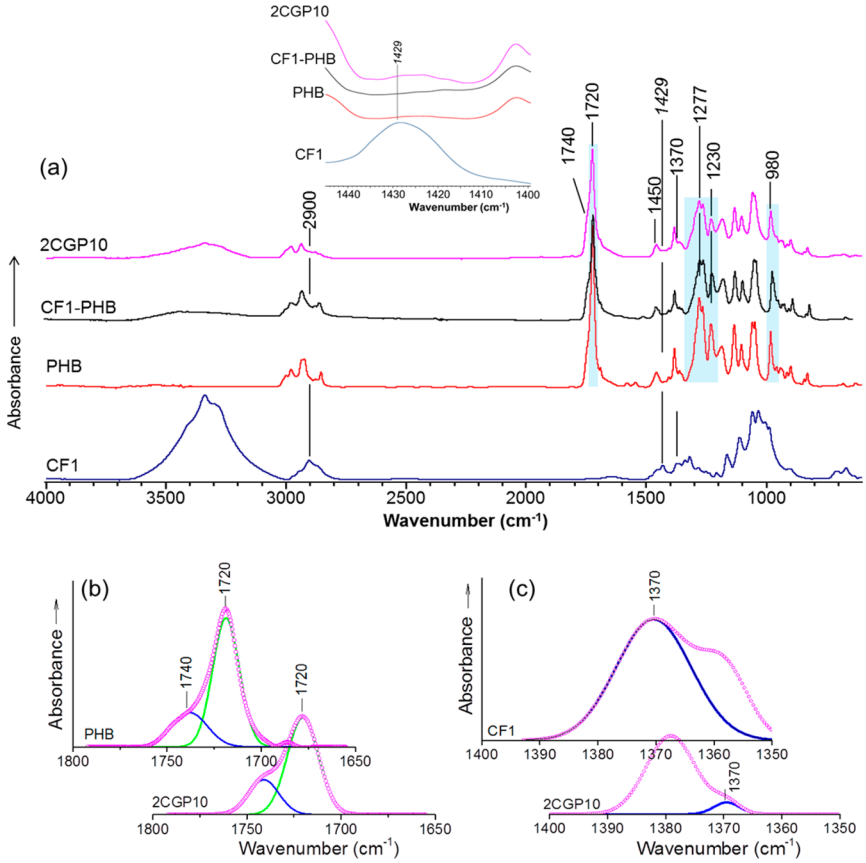

Figure 8. (a) Full and expanded region FTIR spectra for CF1, PHB, CF1-PHB blend, and CF1-*g*-PHB (2CGP10); (b) carbonyl (C═O) fitted peaks for PHB and CF1-g-PHB (2CGP10); and (c) −C−H bending (1370 cm^{-1}) fitted peaks for CF1 and CF1-g-PHB (2CGP10).

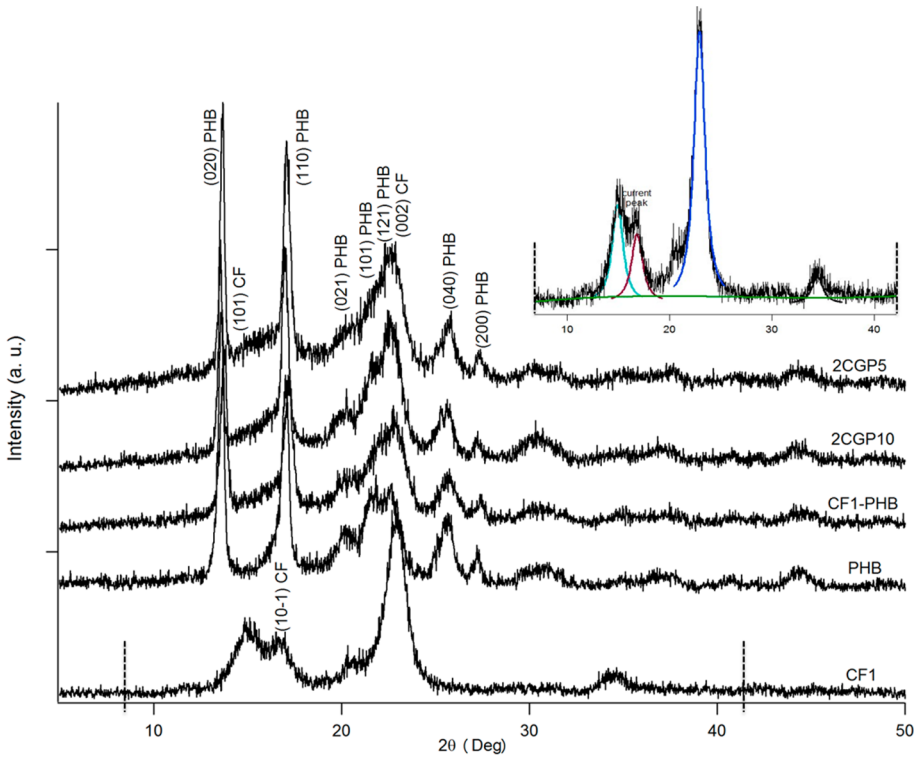

Figure 9. XRD diffractograms of CF1, PHB, CF1-PHB blend, and CF1-*g*-PHB (2CGP5 and 2CGP10) samples. The inset plot shows an example (CF1) of peak fitting using IGOR Pro.

DOI: 10.1021/acs.biomac.5b00049
Biomacromolecules 2015, 16, 1040−1049

Scheme 2. Schematic Illustration of (a) Possible Structures Showing Radicals Formed of CF1 and PHB Melts, and (b) Possible Structure Showing Grafted Sites (Crystalline/Amorphous) between CF1 and PHB of CF1-*g*-PHB[a]

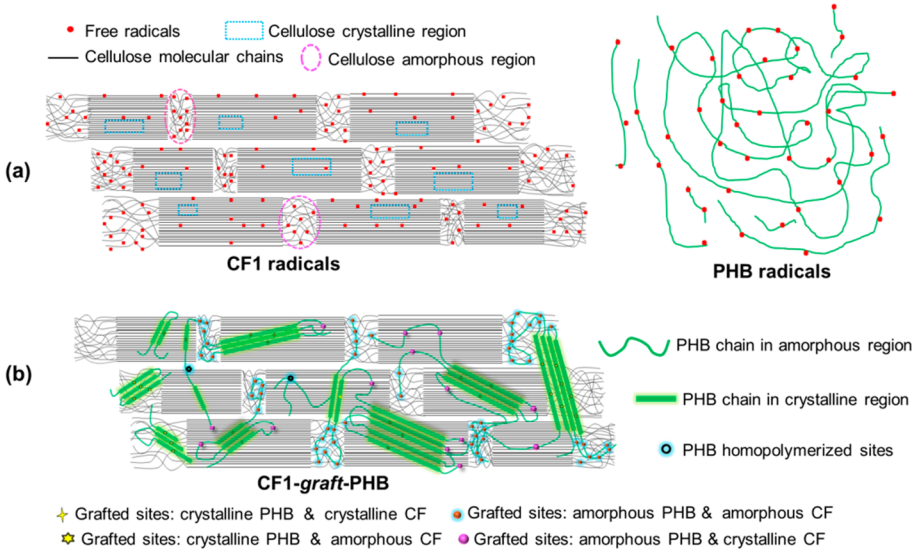

[a]Note: PHB molecular chains with fewer grafted sites tend to crystallize from melt.

and CF1-*g*-PHB products (2CGP5 and 2CGP10) only with lower intensity as compared to native cellulose and PHB. A similar behavior has been observed for bacterial cellulose and PHB composite membrane in that the cellulose and PHB crystallinity were shown to affect each other.[39] The Gaussian function was used for peak fitting of the XRD diffractograms, and therefore, the fwhm values were obtained accordingly. Crystallinity indices were calculated from the ratios of fitted peak intensities, and crystal sizes according to Scherrer's formula using a shape constant $K = 0.9$ for both PHB and cellulose. These parameters can be found in Table S4 (available in the Supporting Information). Crystallinity index and average crystal width were 69% (CrI_{CF1}) and 267 Å (D_{002}) for CF1, and 62% (CrI_{PHB}) and 1309 Å (D_{020}) for PHB, respectively. For the CF1-PHB blend both the CF1 and PHB components showed lower crystallinity indices and crystal sizes. After grafting both crystallinity indices and crystal dimensions were reduced significantly and varied with grafting time (or efficiency) as highlighted between samples 2CGP5 and 2CGP10. This is consistent with the findings from FTIR and DSC analyses, which therefore further confirmed the crystallinity of PHB and cellulose were both reduced during this grafting approach. Smaller crystal sizes of the grafted products suggests that the formation of large crystals of either PHB or cellulose was hindered by each other, because the large crystal size of PHB was one of the most accepted reasons leading to its brittleness.[40] The decrease in cellulose crystallinity in sample 2CGP10 may be caused by the disruption of surface chains of the crystalline regions due to formation of radicals and reaction with PHB. To note, the CF1-PHB blend also had lower PHB and CF1 crystallinity, which may be due to the hindrance of crystallization between them or the amorphous components of both cellulose and PHB with 2θ near to 17°. The similar trend was observed in bacterial cellulose and PHB composites.[39] Nevertheless, the decreasing trend was more significant as a result of grafting suggesting that the grafted sites (C−C bonding) could limit the numbers of PHB chains involved in crystallization except for the physical interruption between them. It is therefore speculated that a limited number of peroxide radicals formed on surfaces of the crystalline phase of CF1 could be attached by PHB, resulting in a higher proportion of amorphous CF1.

Based on the crystallinity changes, the possible grafted sites of CF1-*g*-PHB are proposed: (a) CF1 and melted PHB radicals are produced first (Scheme 2a); (b) the radicals tend to be combined at the possible grafted sites and meantime PHB will crystallize when cools (Scheme 2b). These grafted sites would impede or limit the crystallization of PHB from melts; thus, molecular chains with fewer grafted sites would crystallize when cooled from melts and accounted for the crystalline fraction, whereas molecular chains with more grafted sites would contribute to the amorphous component due to inhibited crystallization. As for CF1, the highly crystalline material with less mobility, only radicals generated on its surface of the crystalline and amorphous regions would be accessible to the molten PHB (with radicals) would be able to produce the CF1-*g*-PHB copolymer. Hence, the grafting density was higher in the CF1 amorphous region. In addition, those grafted sites located on the surfaces of crystalline CF1 would also reduce the crystallinity index of the resultant CF1-*g*-PHB, which agrees with the SEM finding that peroxide treated CF1 surfaces looked different with the original cellulose.

■ CONCLUSIONS

In situ radical initiation via reaction extrusion of PHB was able to graft onto cellulose in a simple process. This "grafting-onto" strategy gave a reasonable grafting efficiency and the grafting efficiency (density) and copolymer composition were dependent on the reaction time and DCP concentration. The highest yield of grafted copolymer was obtained in 5 min with 2% DCP. ESR was used to confirm the presence of radical species on PHB-cellulose materials. The sites of grafting between PHB and cellulose were supported by NMR and confirmed the reaction mechanism as proposed from ESR findings. SEM indicated that the grafting reaction occurred between the surfaces of cellulose and PHB. Due to new bonds formed via grafting the thermal stability of PHB was improved. The crystallinity of the cellulose-PHB material was modified

DOI: 10.1021/acs.biomac.5b00049
Biomacromolecules 2015, 16, 1040−1049

through grafting, which could introduce more flexibility to both cellulose and PHB. The properties of the CF1-*g*-PHB materials (crystallinity and thermal stability) could be tuned by varying reaction conditions. This approach afforded cellulose reinforced Bioplastic composite materials with improved properties by chemically linking the fibers with the matrix to improve stress transfer. This simple reactive extrusion process broadens the processing window for PHB and PHB-based biocomposites and, ultimately, the applications these biomaterials can be used such as packaging and semistructural profiles.

■ ASSOCIATED CONTENT

Supporting Information

Conditions for PHB and cellulose treatment and reaction parameters (Table S1), grafting parameters (e.g., %GP, %GE, and %WC; Table S2), DSC results (Table S3), crystallinity parameters (Table S4), and ^{13}C NMR spectrum of as received PHB (Figure S1). Figure S1: ^{13}C NMR spectrum of PHB. Note: the signals shown at δ = 38.9 and 27.1 ppm are from impurities of commercial PHB used. This material is available free of charge via the Internet at http://pubs.acs.org.

■ AUTHOR INFORMATION

Corresponding Author

*E-mail: armandm@uidaho.edu. Tel.: +1 (208) 885 9454. Fax: +1 (208) 885 6226.

Notes

The authors declare no competing financial interest.

■ ACKNOWLEDGMENTS

The authors would like to acknowledge (i) the financial support from a USDA-Forest Products Laboratory Grant 08-JV-111111, (ii) Dr. Alexander Blumenfeld for his technical help with ESR and NMR, (iii) USDA-CSREES Grant 2007-34158-17640 for supporting the DSC, and (iv) ThermoScientific for the FTIR spectrometer.

■ REFERENCES

(1) Carlmark, A.; Larsson, E.; Malmström, E. *Eur. Polym. J.* **2012**, *48*, 1646−1659.
(2) Roy, D.; Semsarilar, M.; Guthrie, J. T.; Perrier, S. *Chem. Soc. Rev.* **2009**, *38*, 2046.
(3) Kadla, J. F.; Gilbert, R. D. *Cell. Chem. Technol.* **2000**, 197−216.
(4) Klemm, D.; Heublein, B.; Fink, H.-P.; Bohn, A. *Angew. Chem., Int. Ed.* **2005**, *44*, 3358−3393.
(5) Nishino, T.; Matsuda, I.; Hirao, K. *Macromolecules* **2004**, *37*, 7683−7687.
(6) Wambua, P.; Ivens, J.; Verpoest, I. *Compos. Sci. Technol.* **2003**, *63*, 1259−1264.
(7) Wittek, T. *Express Polym. Lett.* **2008**, *2*, 810−822.
(8) Habibi, Y.; Goffin, A.-L.; Schiltz, N.; Duquesne, E.; Dubois, P.; Dufresne, A. *J. Mater. Chem.* **2008**, *18*, 5002−5010.
(9) Lönnberg, H.; Zhou, Q.; Brumer, H., III; Teeri, T. T.; Malmström, E.; Hult, A. *Biomacromolecules* **2006**, *7*, 2178−2185.
(10) Zoppe, J. O.; Habibi, Y.; Rojas, O. J.; Venditti, R. A.; Johansson, L.-S.; Efimenko, K.; Österberg, M.; Laine, J. *Biomacromolecules* **2010**, *11*, 2683−2691.
(11) Liu, S.; Sun, G. *Carbohydr. Polym.* **2008**, *71*, 614−625.
(12) Oh, J. K.; Lee, D. I.; Park, J. M. *Prog. Polym. Sci.* **2009**, *34*, 1261−1282.
(13) Gupta, K. C.; Khandekar, K. *Biomacromolecules* **2003**, *4*, 758−765.
(14) Gupta, K. C.; Sahoo, S.; Khandekar, K. *Biomacromolecules* **2002**, *3*, 1087−1094.
(15) Chen, G.-Q.; Wu, Q. *Biomaterials* **2005**, *26*, 6565−6578.
(16) Chen, G.-Q.; Patel, M. K. *Chem. Rev.* **2012**, *112*, 2082−2099.
(17) Mekonnen, T.; Mussone, P.; Khalil, H.; Bressler, D. *J. Mater. Chem.* **2013**, *1*, 13379−13398.
(18) Wei, L.; McDonald, A. G. *J. Appl. Polym. Sci.* **2015**, *132*, 4233−4247.
(19) Samain, X.; Langlois, V.; Renard, E.; Lorang, G. *J. Appl. Polym. Sci.* **2011**, *121*, 1183−1192.
(20) Segal, L.; Creely, J. J.; Martin, A. E.; Conrad, C. M. *Text. Res. J.* **1959**, *29*, 786−794.
(21) Alexander, L. E. *X-ray Diffraction Method in Polymer Science*; Wiley-Interscience: New York, 1969.
(22) Wei, L.; McDonald, A. G.; Freitag, C.; Morrell, J. J. *Polym. Degrad. Stab.* **2013**, *98*, 1348−1361.
(23) Dannenberg, E. M.; Jordan, M. E.; M, H. *J. Polym. Sci.* **1958**, *31*, 127−153.
(24) Arslan, H.; Hazer, B.; Yoon, S. C. *J. Appl. Polym. Sci.* **2007**, *103*, 81−89.
(25) Zhou, W.; Zhu, S. *Ind. Eng. Chem. Res.* **1997**, *36*, 1130−1135.
(26) Takamura, M.; Nakamura, T.; Takahashi, T.; Koyama, K. *Polym. Degrad. Stab.* **2008**, *93*, 1909−1916.
(27) Saiki, S.; Nagasawa, N.; Hiroki, A.; Morishita, N.; Tamada, M.; Kudo, H.; Katsumura, Y. *Radiat. Phys. Chem.* **2011**, *80*, 149−152.
(28) VanderHart, D. L.; Hyatt, J. A.; Atalla, R. H.; Tirumalai, V. C. *Macromolecules* **1996**, *29*, 730−739.
(29) Hon, D. N.-S.; Shiraishi, N. *Wood and Cellulosic Chemistry*, 2nd ed., revised and expanded; Marcel Dekker, Inc.: New York, 2001.
(30) Joseph, K.; Thomas, S. *Polymer* **1996**, *37*, 5139−5149.
(31) Wei, L.; Guho, N. M.; Coats, E. R.; McDonald, A. G. *J. Appl. Polym. Sci.* **2014**, *131*, 5516−5528.
(32) Kurniawan, L.; Qiao, G. G.; Zhang, X. *Biomacromolecules* **2007**, *8*, 2909−2915.
(33) Bengtsson, M.; Gatenholm, P.; Oksman, K. *Compos. Sci. Technol.* **2005**, *65*, 1468−1479.
(34) Qiu, Z.; Ikehara, T.; Nishi, T. *Polymer* **2003**, *44*, 3095−3099.
(35) Xu, J.; Guo, B.; Yang, R.; Wu, Q.; Chen, G.; Zhang, Z. *Polymer* **2002**, *43*, 6893−6899.
(36) Åkerholm, M.; Hinterstoisser, B.; Salmén, L. *Carbohydr. Res.* **2004**, *339*, 569−578.
(37) Yu, H.-Y.; Qin, Z.-Y.; Wang, L.-F.; Zhou, Z. *Carbohydr. Polym.* **2012**, *87*, 2447−2454.
(38) Medvecky, L. *Sci. World J.* **2012**, *2012*, 1−8.
(39) Barud, H. S.; Souza, J. L.; Santos, D. B.; Crespi, M. S.; Ribeiro, C. A.; Messaddeq, Y.; Ribeiro, S. J. L. *Carbohydr. Polym.* **2011**, *83*, 1279−1284.
(40) De Koning, G. J. M.; Lemstra, P. J. *Polymer* **1993**, *34*, 4089−4094.

DOI: 10.1021/acs.biomac.5b00049
Biomacromolecules 2015, 16, 1040−1049